Supporting Information

Macro-mesoporous carbon architectures for confining sulfur and facilitating Li^+ transport in high-performance Li-S batteries

Huanyu Zhang,[a] *and Limin Huang*[a,]*

[a] Department of Chemistry, Southern University of Science and Technology,

Shenzhen 518055, P.R. China

* Corresponding author. E-mail: huanglm@sustech.edu.cn

Experimental section

Chemicals and Materials

All reagents were used as received without further purification. Lithium foil (99.9 wt%, 0.6 mm thick), sublimed sulfur (>99.5 wt%), lithium sulfide (99.98%, Li_2S), ethanol (>99 wt%, anhydrous), acetic acid (36 wt%), nickel chloride hexahydrate (98 wt%), cobalt chloride hexahydrate (98 wt%), urea (99 wt%) and furfuryl alcohol (98 wt%) were supplied by Aladdin. The zinc-manganese batteries from NanFu AA brand were already used. The Li-S battery electrolyte was a 1.0 M lithium bis(trifluoromethanesulfonyl)imide (LiTFSI) + 5 wt% $LiNO_3$ solution in DOL/DME (1:1 v/v) from DoDoChem in SuZhou, China.

Recyclable Process of Preparation of NiCo-HPNC

First, the used zinc-manganese batteries were completely disassembled. The main component of the anode material was detected as ZnO by XRD. After drying and grinding, the anode material (2.03 g) of zinc-manganese batteries was dissolved in acetic acid (20 mL). The mixture was heated and stirred until the majority of it had dissolved. Insoluble substances were then filtered out. The reaction was carried out in a 130 ℃ oil bath for 30 minutes, followed by continued heating to concentrate the solution, leading to crystallization. The product obtained (3.78 g) was identified as zinc acetate by XRD. The zinc acetate nanoparticles can serve as a template for HPC preparation. Next, furfuryl alcohol (FA) was infiltrated into the gaps of the tightly packed $Zn(OAc)_2$. Meanwhile, nitrogen doping and the incorporation of transition metals into porous carbon structures can be simultaneously achieved through a one-pot

synthesis approach. The ZnO generated during the process can be dissolved again into $Zn(OAc)_2$ solution using acetic acid in a 130 ℃ oil bath. Continue heating the acetic acid solution and crystallizing to obtain zinc acetate crystals. The zinc acetate crystals can then be used again, enabling the cyclic utilization of the initial waste materials from the used zinc-manganese batteries. Finally, the NiCo-HPNC cathode was obtained, aligning with the concept of environmental sustainability.

One-pot Preparation of NiCo-HPNC

Dissolve urea (462.5 mg), cobalt chloride hexahydrate (224.5 mg) and nickel chloride hexahydrate (225.2 mg) in furfuryl alcohol solution (5 mL) in advance under magnetic stirring for 30 min at 60 °C. Then the solution was sonicated for 10 min and added to $Zn(OAc)_2$ template (15.0 g). The mixture was centrifuged at 10000 rpm for 10 min, and the excess clear supernatant was carefully removed. Subsequently, it was heated at 90 °C for 6 h to ensure complete polymerization. The powder was subsequently heated to 300 °C (heating rate, 5 °C min^{-1}) for 5 h in an argon flow. The obtained powder was washed thoroughly by 1:1 v/v mixture of deionized water and anhydrous ethanol and then dried in an oven at 80 °C. Next, the powder was heated to 550 °C (heating rate, 2 °C min^{-1}) and held for 5 h in an argon flow, immediately followed by an elevated temperature of 900 ℃ (heating rate, 10 ℃ min^{-1}) and held for 2 h. After cooling to room temperature, the sample was added to the acetic acid solution, sealed and stirred at 500 rpm while heating to 130 ℃. The suspension was separated by centrifugation at 9000 rpm and washed with acetic acid three times. Finally, the NiCo-HPNC product was dried at 60 °C overnight in a vacuum.[1]

One-pot Synthesis of HPNC

Dissolve urea (462.5 mg) in furfuryl alcohol solution (5 mL) in advance. The following steps are consistent with the process of synthesizing NiCo-HPNC, except that the transition metals Ni and Co were not introduced.

Synthesis of NC

Dissolve urea (462.5 mg) in furfuryl alcohol solution (5 mL) in advance. The solution was then polymerized and pyrolyzed directly without the $Zn(OAc)_2$ template. The temperature program was identical to that used for NiCo-HPNC, without the addition of Ni and Co precursors.

Fabrication of Freestanding Cathodes

NiCo-HPNC/HPNC/NC (120 mg) was dispersed in anhydrous ethanol (120 mL) and ultrasonicated for 2 h. Thereafter, the solution was vacuum-filtered through the organic membrane filter. The membrane filter was then vacuum-dried at 60 °C overnight. A freestanding electrode film could be easily peeled off the membrane filter. Each electrode film was prepared to a weight of 17 mg. Freestanding electrodes were obtained without a collector and PVDF.

Preparation of Electrolyte

1 M Li_2S_6 solution: 6 mmol Li_2S and 30 mmol sublimed sulfur were added to 6 mL of 1 M LiTFSI + 5 wt% $LiNO_3$ solution in DOL/DME (1:1 v/v). The mixture was heated at 60 °C under magnetic stirring for 24 h. The color of the solution gradually turned to dark brown. The preparation of the 2 M Li_2S_6 solution is as above, except that the sulfur and lithium sulfide were added twice as much.

Li_2S_6 Symmetric Cell Measurements

A 0.15 M Li_2S_6, 0.5 M LiTFSI and 0.1 M $LiNO_3$ solution in tetraglyme was prepared and used as electrolyte. For the assembly of symmetric cells, two identical electrodes were assembled into a standard 2025-coin cell. 40 μL of electrolyte was added to each cell. Cyclic voltammetry (CV) measurements of these symmetric cells were carried out at a scan rate of 0.2 mV s^{-1} between -1.0 and 1.0 V.

Lithium Polysulfide (LiPSs) Adsorption Test

A 5 mM Li_2S_6 solution was prepared by completely dissolving Li_2S and S with a molar ratio of 1:5 in a stoichiometric ratio in 1, 2-dimethoxyethane (DME) in an argon-filled glove box. After that, 10 mg of NC, HPNC and NiCo-HPNC were respectively added into 5 mmol L^{-1} Li_2S_6/DME solution that was stood for 6 h.

Li_2S Deposition Measurements

A polysulfide (0.2 M Li_2S_8) solution was prepared by mixing 0.4 mmol Li_2S, 2.8 mmol S and 2 mmol LiTFSI in 2 mL tetraglyme at 50 °C for 8 h. Then the Li_2S_8 catholyte was dropped onto the cathodes. 20 μL blank electrolyte without the Li_2S_8 was added to the anode compartment. The assembled cells were first discharged galvanostatically to 2.06 V at a constant current density of 0.112 mA, and then held potentiostatically at 2.05 V until the measured current was below 10^{-5} A.

Li_2S Dissolution Measurements

The cathode after the Li_2S deposition measurement was recovered and re-assembled into a new test cell. The new test cell also contained the blank electrolyte, the Celgard membrane separator, and a Li metal foil anode. The assembled test cell was discharged

galvanostatically to 1.70 V at a very low current value (about 10^{-5} A) and then charged potentiostatically at 2.35 V until the measured current was below 10^{-5} A. The decomposition capacity of Li_2S was estimated from the area under the curve.

Materials Characterization

Morphology examinations of materials were performed by means of TEM (an FEI Tecnai F30 microscope at 300 kV), and SEM (an FEI Nova NanoSem 450). XRD patterns were collected by a Rigaku SmartLab system (45 kV and 200 mA) using Cu Kα radiation (LKα1= 1.540593 Å, LKα2= 1.544414 Å). The adsorption of polysulfides on various substrates was evaluated with a UV–vis absorption spectrophotometer (PerkinElmer LAMBDA 750s). Li-S coin cells were assembled in a stainless-steel setup with a quartz window on top for in-situ Raman spectroscopy (LabRAM HR Evolution) investigation with a 532 nm laser. Each spectrum was acquired for 20 s. The batteries were cycled at the 0.2 C rate, and spectra were collected per 15 min.

Electrochemical Characterization

CR2025-type coin cells were assembled in an Ar-filled glove box with the self-standing cathode, a lithium foil anode and a Celgard 2325 polypropylene membrane separator. Li_2S_6 catholyte was the sulfur source, and a 1.0 M LiTFSI solution in DOL/DME (1:1, v/v) with 5 wt% $LiNO_3$ was the electrolyte. The wetted electrode area was about 1.5 cm^2. The sulfur loading in the electrochemical tests depended on the amount of the Li_2S_6 solution and was in the range of 6.2–12.4 mg cm^{-2}. The electrolyte to sulfur ratio (E/S) in the coin cells was ≈ 4.8 μL mg^{-1}. All batteries were assembled in an Ar-filled glove box. A NEWARE BTS-5 V battery instrument was used to perform

charge/discharge testing in a voltage range of 1.7–2.8 V at room temperature. A PARSTAT 4000+ electrochemical workstation was used for cyclic voltammetry and electrochemical impedance spectroscopy testing. All measurements were carried out at room temperature. Tafel plots were employed to describe the relationship between current density and overpotential. Through linear fitting, the Tafel slope can be obtained, which allows analysis of the electrode-reaction kinetics and catalyst activity. The tests were performed in full-cell configuration with a voltage scan range from 1.80 V to 2.70 V at a scan rate of 6 mV s^{-1}. The cathodes used were freestanding NiCo-HPNC, HPNC, and NC electrodes, while lithium foil served as the anode. The electrode geometric area was 1 cm^2.

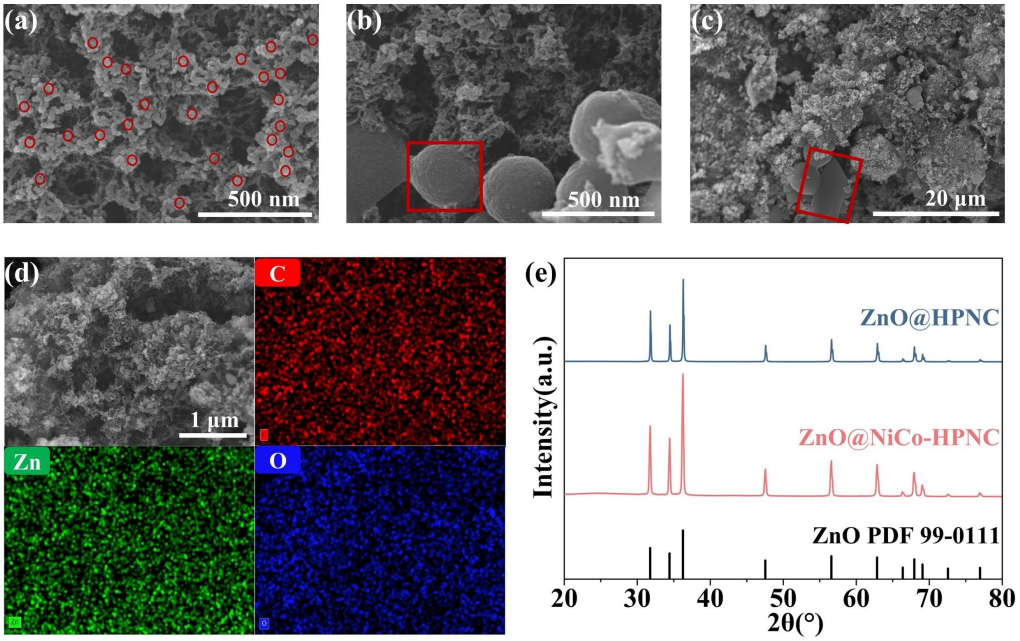

Figure S1. (a-c) SEM images of ZnO@NiCo-HPNC at various magnifications (Three distinct morphologies of ZnO are highlighted in red). (d) EDS elemental mapping (C, Zn, O). (e) XRD patterns of ZnO@HPNC and ZnO@NiCo-HPNC.

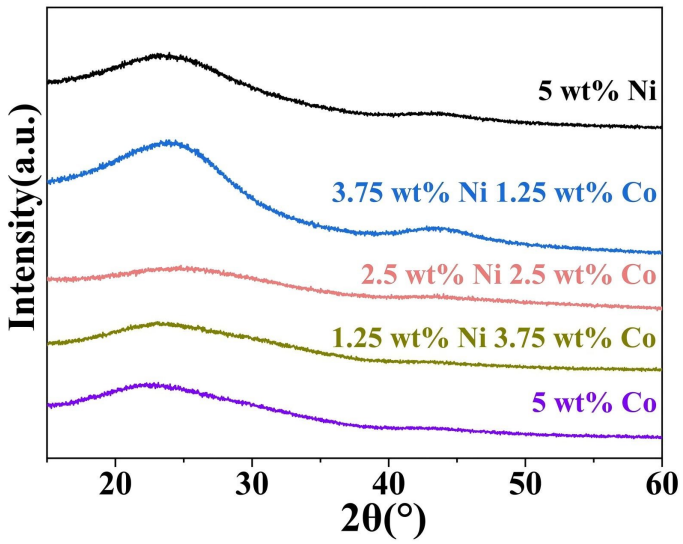

Figure S2. XRD patterns of NiCo-HPNC doped with different NiCo contents.

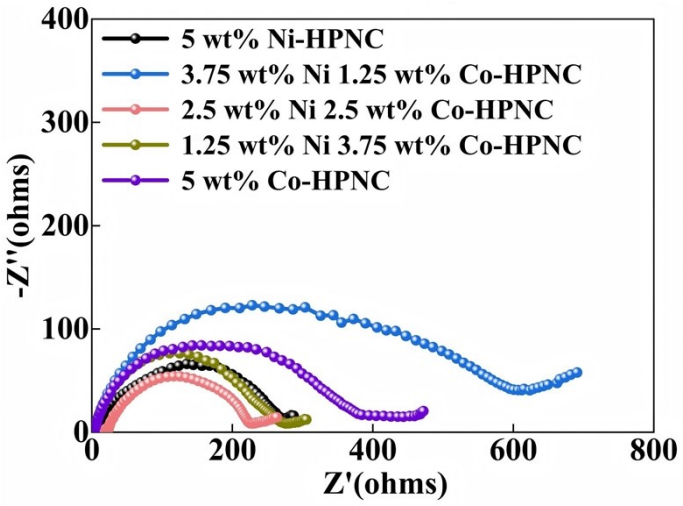

Figure S3. EIS spectra with NiCo-HPNC cathodes doped with different NiCo contents.

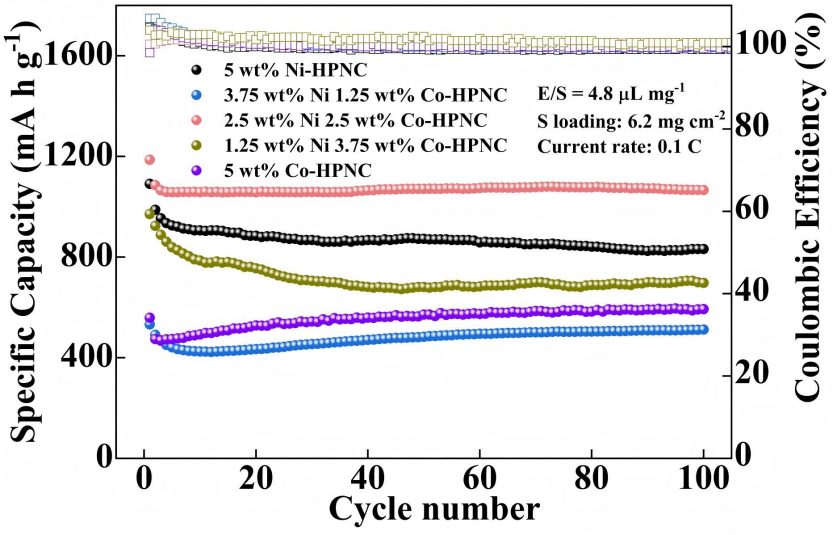

Figure S4. Cycling performance with high S loading at 0.1 C for NiCo-HPNC cathodes doped with different NiCo contents.

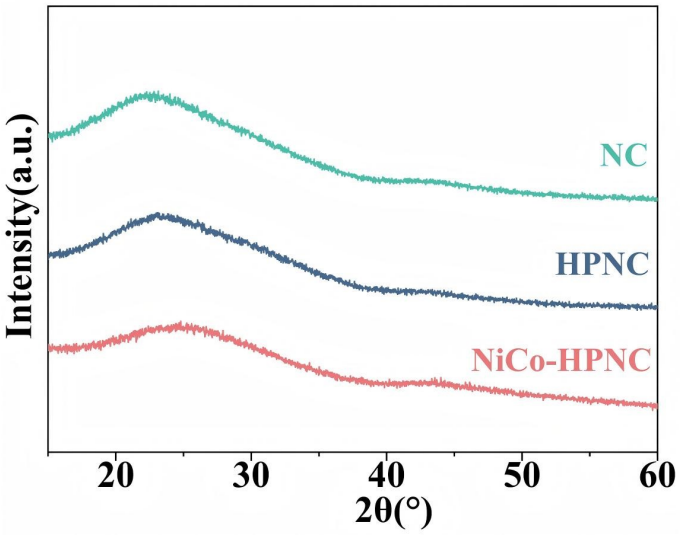

Figure S5. XRD patterns of NC, HPNC and NiCo-HPNC.

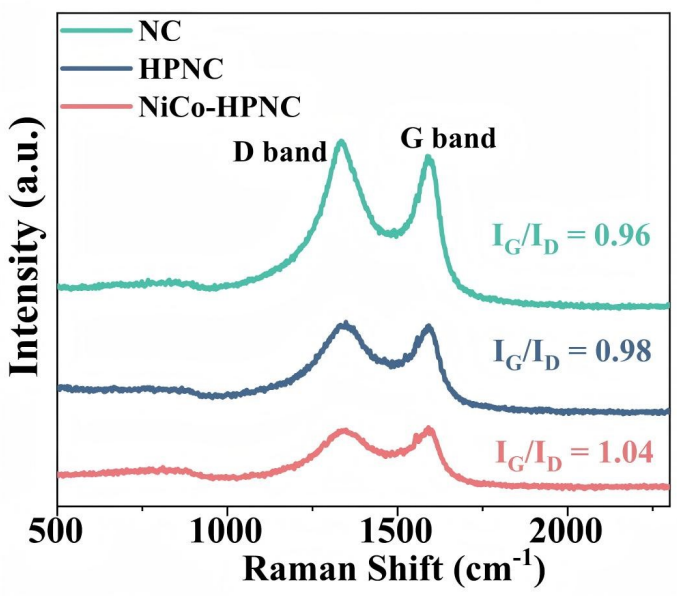

Figure S6. Raman spectra of NC, HPNC and NiCo-HPNC.

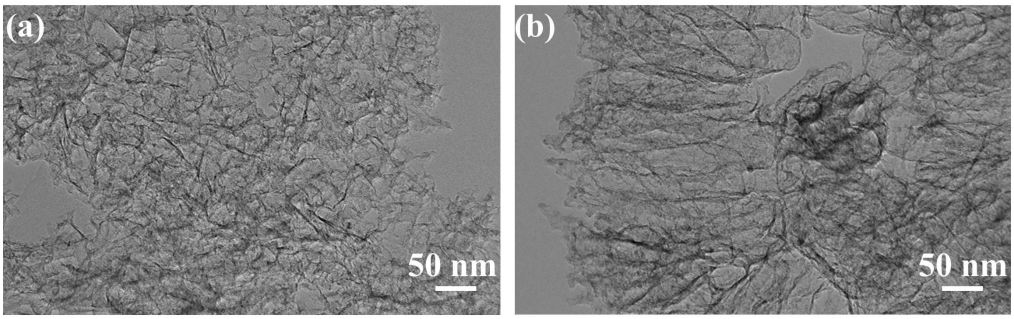

Figure S7. (a-b) TEM images of NiCo-HPNC (scale bar: 50 nm).

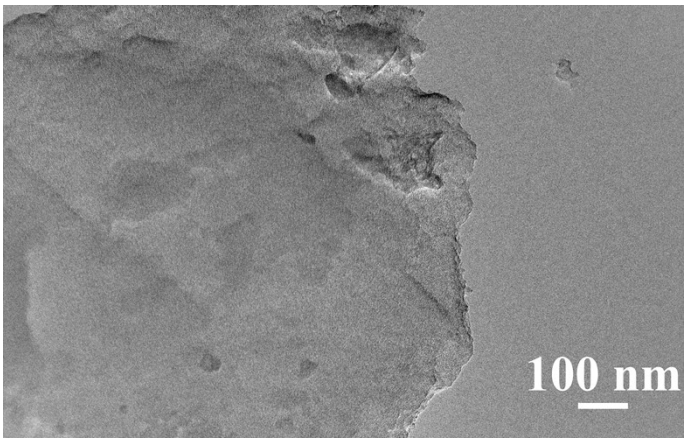

Figure S8. The TEM morphology of NC produced from PFA without template.

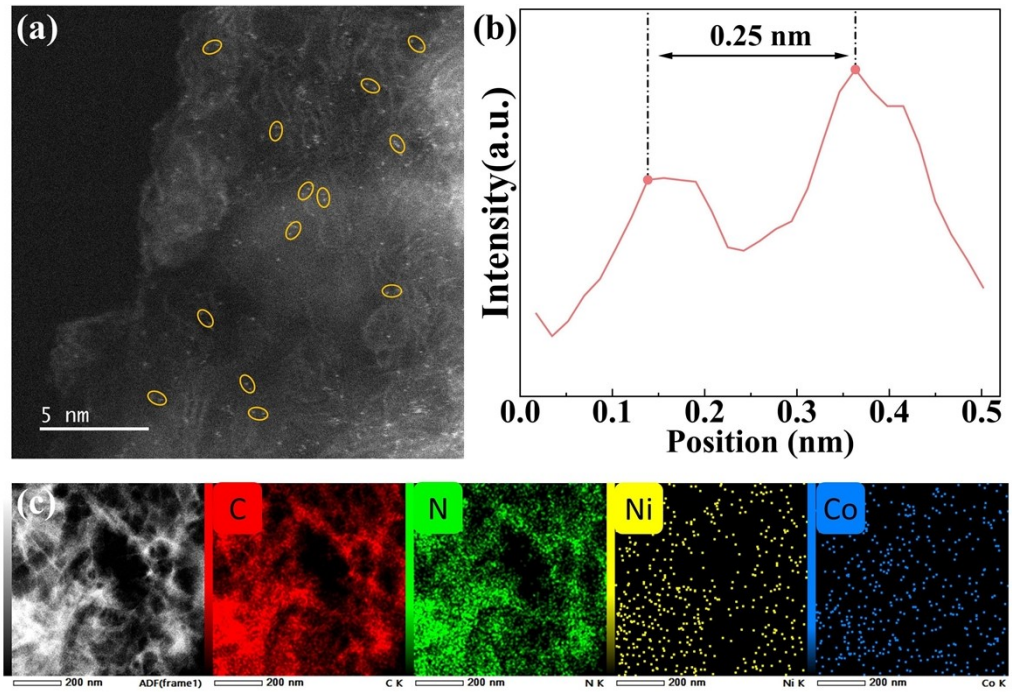

Figure S9. (a) Aberration-corrected HAADF-STEM images of NiCo-HPNC (The dual-atom sites are highlighted with yellow circles). Scale bar: 5 nm. (b) The line scan of the dual-atom site. (c) HAADF images and corresponding EDS mapping of NiCo-HPNC.

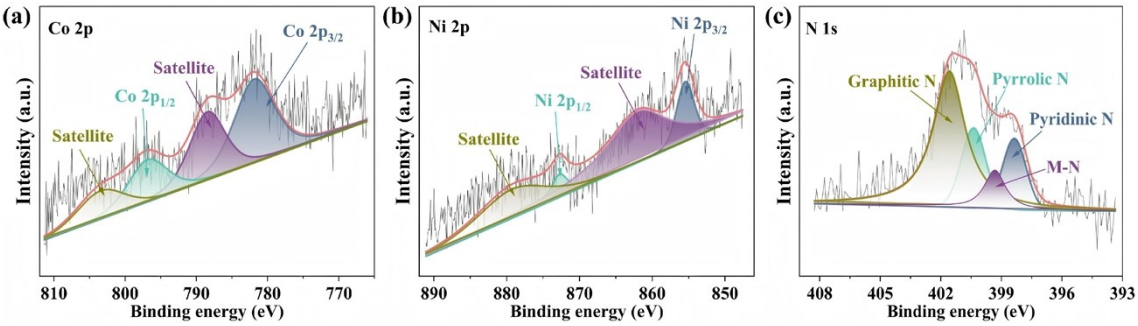

Figure S10. High-resolution XPS spectra of NiCo-HPNC. (a) Co 2p. (b) Ni 2p. (c) N 1s.

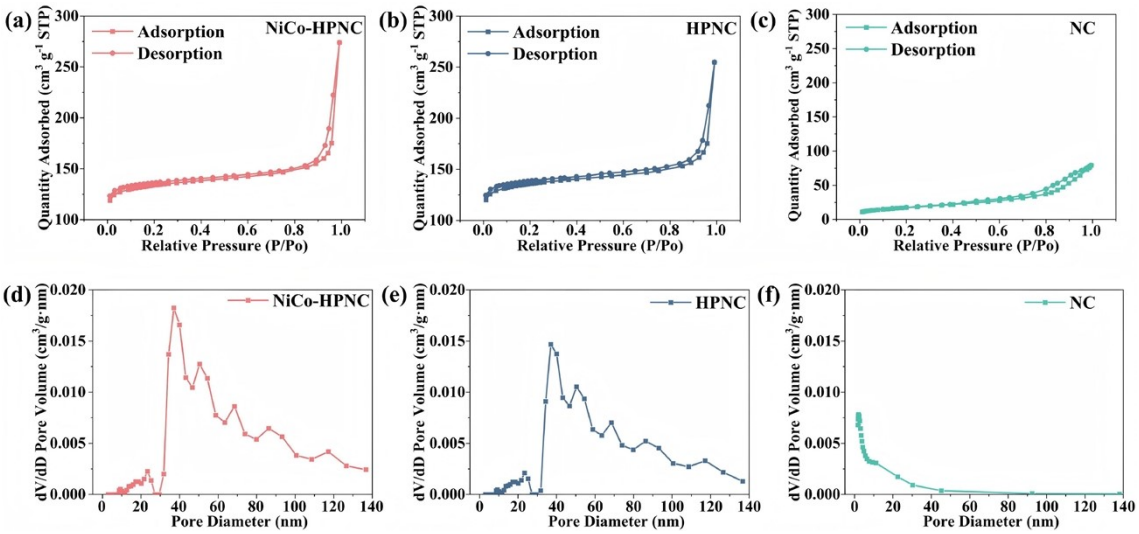

Figure S11. (a-c) N_2 adsorption-desorption isotherms of NiCo-HPNC, HPNC and NC. (d-f) Pore size distributions of NiCo-HPNC, HPNC and NC.

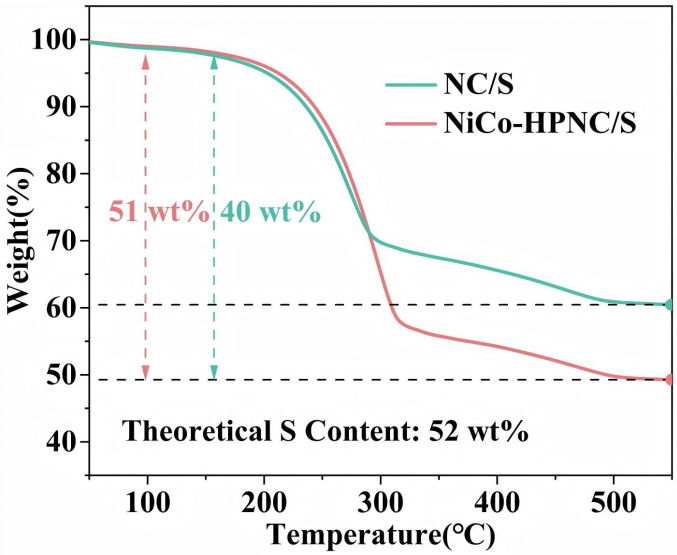

Figure S12. TGA curves of NC/S and NiCo-HPNC/S in N_2 atmosphere.

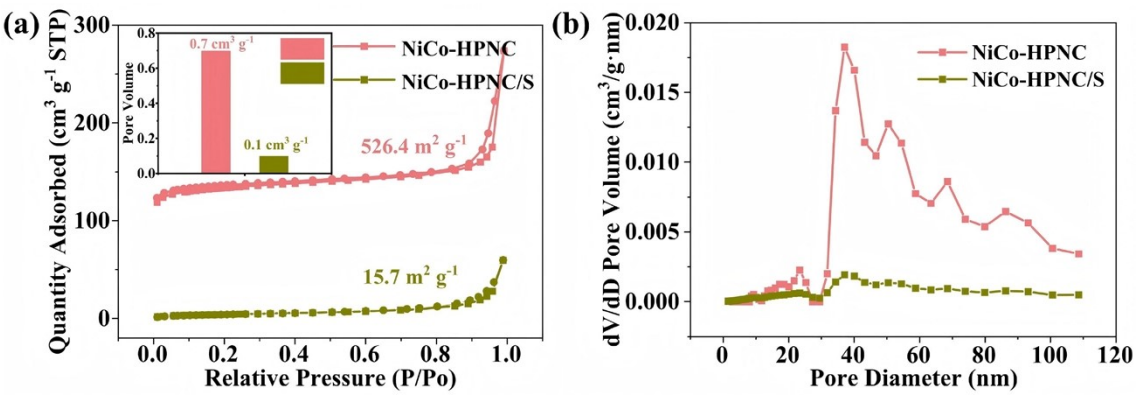

Figure S13. (a) N_2 adsorption-desorption isotherms of NiCo-HPNC and NiCo-HPNC/S (Inset: corresponding pore volume). (b) Pore size distributions of NiCo-HPNC and NiCo-HPNC/S.

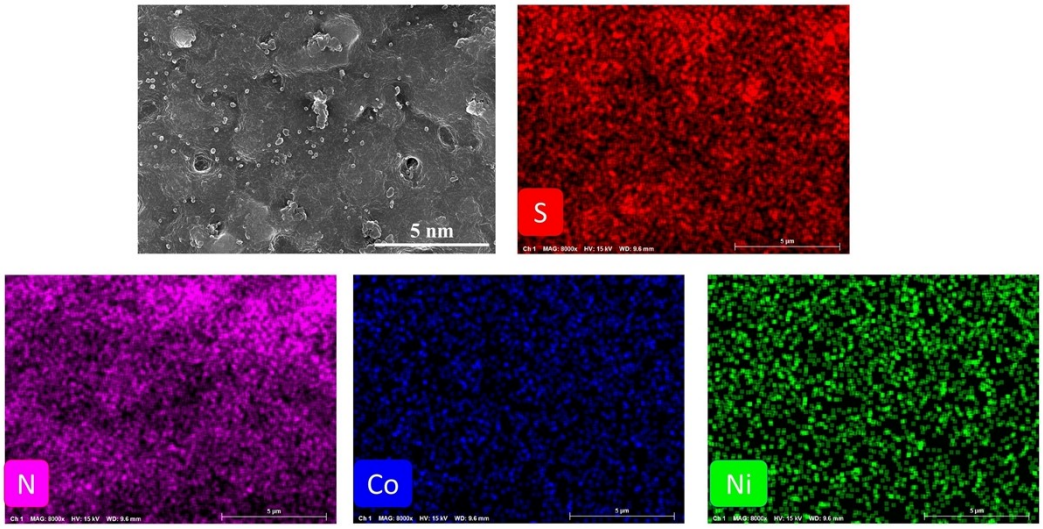

Figure S14. SEM image and corresponding EDS mapping of NiCo-HPNC/S.

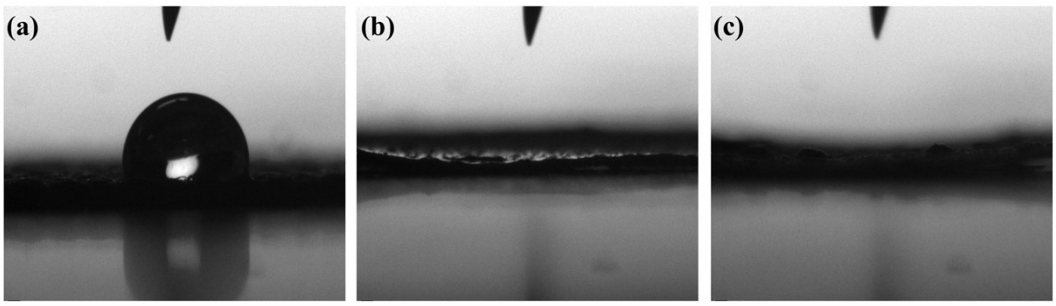

Figure S15. Contact angles of DOL/DME electrolyte on the surfaces of (a) NC, (b) HPNC and (c) NiCo-HPNC.

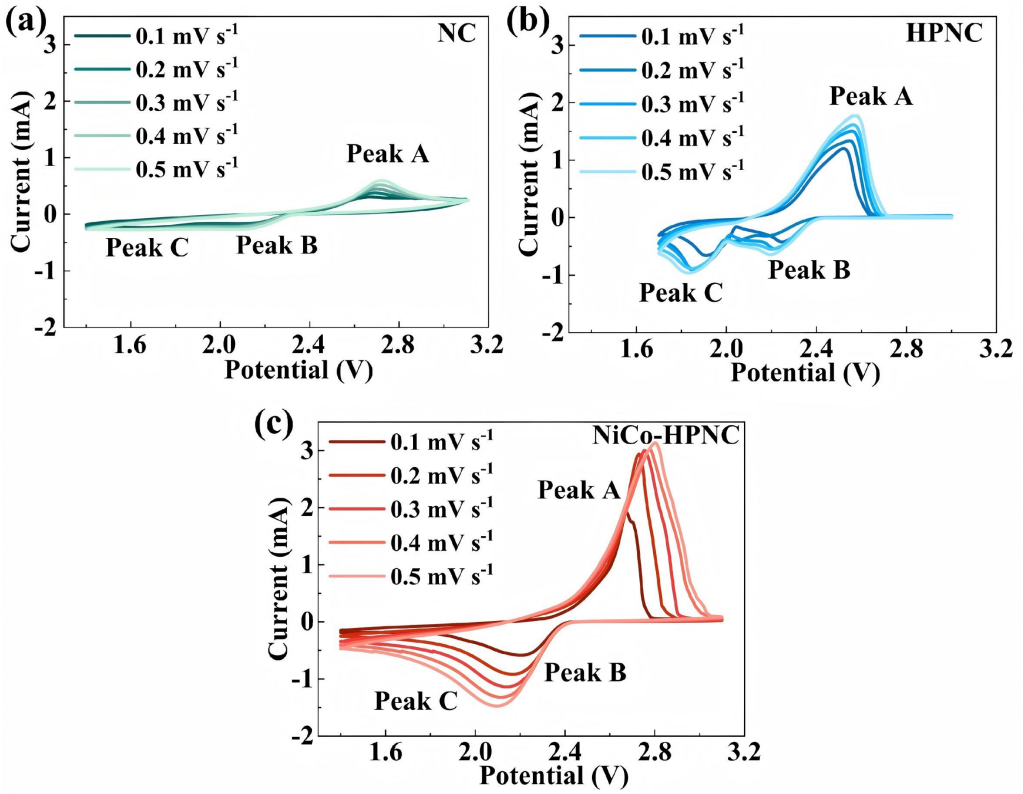

Figure S16. Cyclic voltammetry of (a) NC, (b) HPNC and (c) NiCo-HPNC at different scan rates.

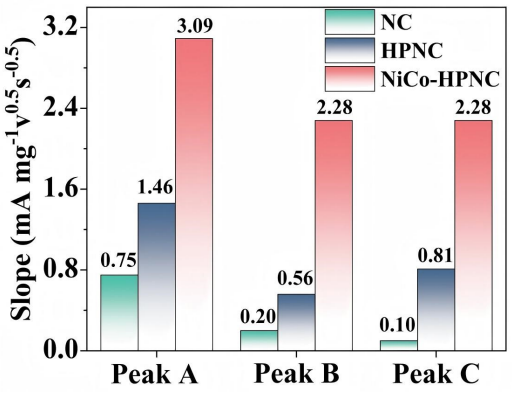

Figure S17. Slope values of different redox peaks of NC, HPNC and NiCo-HPNC.

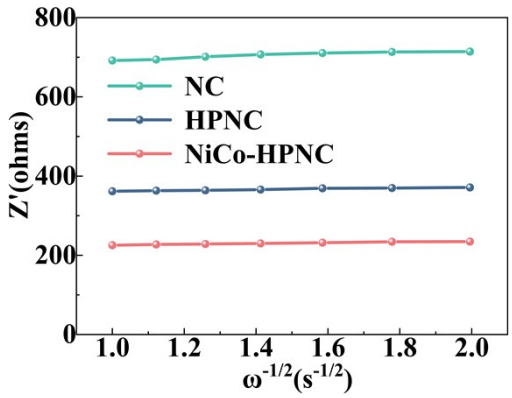

Figure S18. Plots of Z' versus $\omega^{-1/2}$ of NC, HPNC and NiCo-HPNC cathodes.

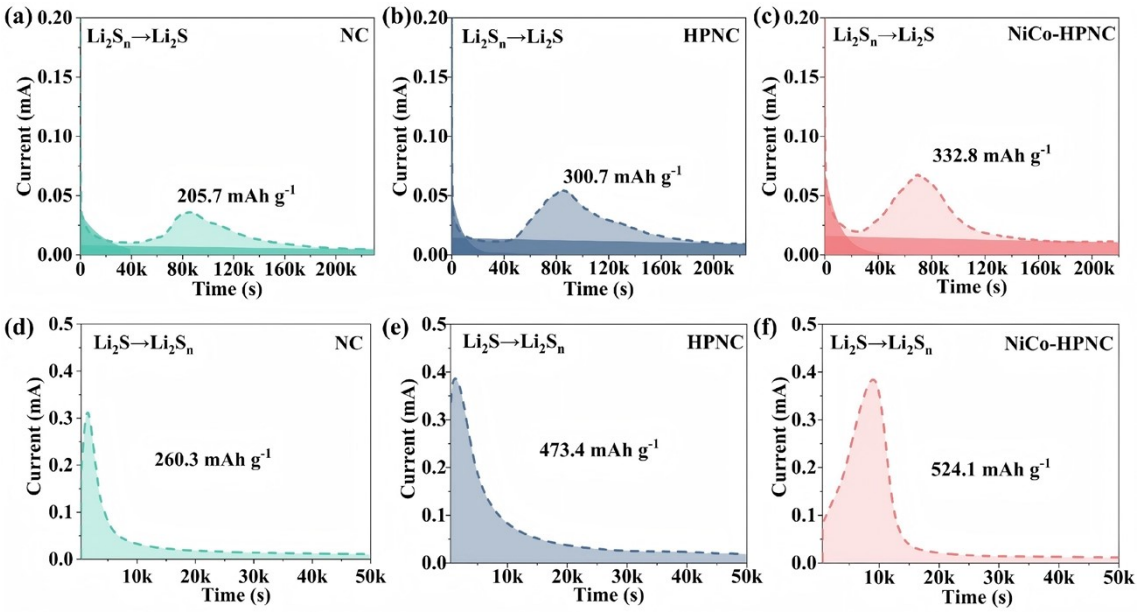

Figure S19. (a-c) Potentiostatic discharge curves of Li_2S deposition on NC, HPNC and NiCo-HPNC. (d-f) Potentiostatic charge curves of Li_2S dissolution on NC, HPNC and NiCo-HPNC.

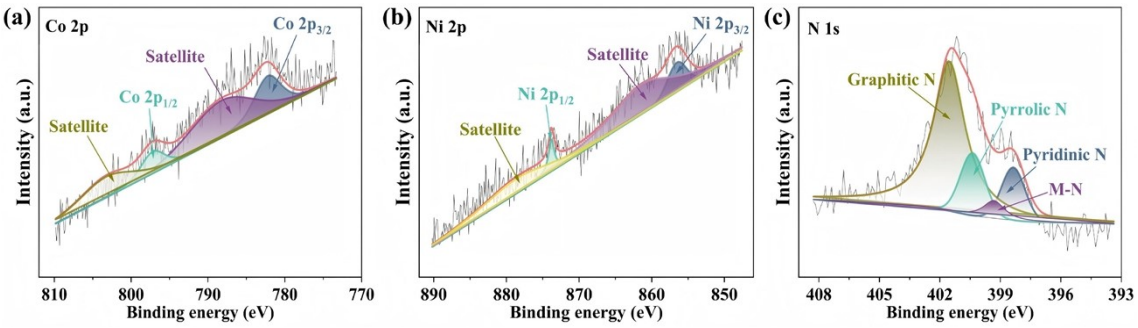

Figure S20. High-resolution XPS spectra of NiCo-HPNC after prolonged cycling. (a) Co 2p. (b) Ni 2p. (c) N 1s.

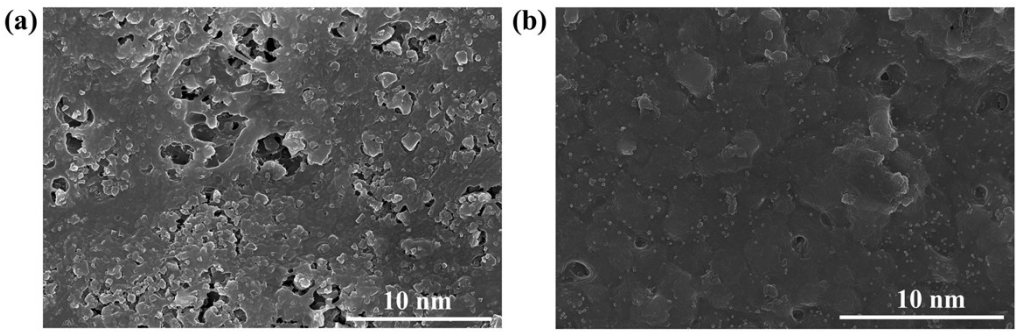

Figure S21. SEM images of (a) the NC cathode and (b) the NiCo-HPNC cathode after the long-term cycling test.

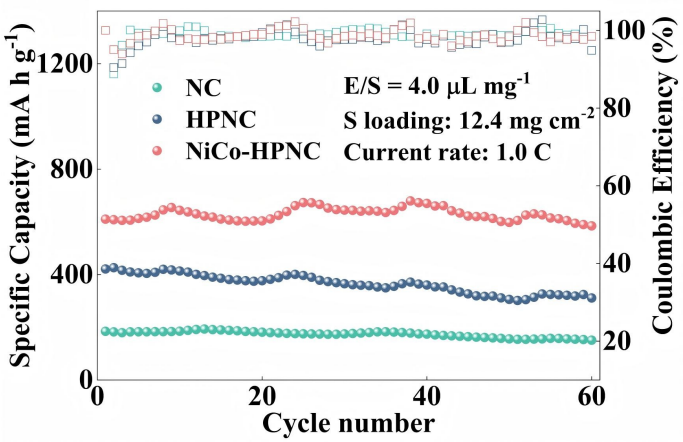

Figure S22. Cycling performance with ultra-high S loading at 1 C.

Equation S1

Randles-Sevcik equation: $$I = 2.686 \times 10^5 n^{1.5} A D_{Li^+}^{0.5} C v^{0.5} \quad (1)$$

where I is the peak current; n the number of electrons; A the electrode area; D_{Li^+} the Li^+ diffusion coefficient; C the Li^+ concentration; and ν the scan rate. D_{Li^+} could therefore be determined from the slope of the linear plot of peak current I vs $v^{0.5}$.

Table S1. Summary of specific surface area, pore volume and volume ratios occupied by different pore types of NC, HPNC and NiCo-HPNC.

Samples	Specific surface area ($m^2 g^{-1}$)	Mesopore size (nm)	Pore volume ($cm^3 g^{-1}$)	Micropores ratio (%)	Mesopores ratio (%)	Macropores ratio (%)
NC	61.9	-	0.11	-	-	-
HPNC	533.9	40~50	0.59	3	30	67
NiCo-HPNC	526.4	40~50	0.74	3	25	72
Microwave C[2]	1459.6	10~20	3.18	2	79	19
Reflux C[2]	747.6	5~10	1.03	3	92	5
Calcination C[2]	1270.6	-	1.42	2	74	24

Table S2. Elemental content in NiCo-HPNC determined by inductively coupled plasma optical emission spectrometry (ICP-OES).

Element	Content (wt%)
Zn	0.01
Co	0.78
Ni	0.75

Table S3. Lithium ion diffusion coefficient (D_{Li^+}) values of the different electrodes

Electrode	D_{Li^+} (cm² s⁻¹)
NC	1.92×10^{-10}
HPNC	6.26×10^{-8}
NiCo-HPNC	9.80×10^{-8}
Microwave C[2]	4.56×10^{-8}
Reflux C[2]	2.50×10^{-8}
Calcination C[2]	3.40×10^{-8}

Table S4. Summary of cycling stability for batteries assembled with different cathodes over 500 cycles at 1C rate.

Samples	Initial discharge capacity (mAh g^{-1})	Final discharge capacity (mAh g^{-1})	Capacity retention rate (%)	Capacity fade per cycle (%)
NC	276.3	160.2	57.9	0.109
HPNC	834.1	533.9	64.0	0.089
NiCo-HPNC	987.0	844.4	85.6	0.031
Microwave C[2]	1223.0	901.0	73.7	0.061
Reflux C[2]	593.4	279.6	47.1	0.151
Calcination C[2]	752.4	412.4	54.8	0.120

References

[1] X. Hai, S. Xi, S. Mitchell, K. Harrath, H. Xu, D. F. Akl, D. Kong, J. Li, Z. Li, T. Sun, H. Yang, Y. Cui, C. Su, X. Zhao, J. Li, J. Pérez-Ramírez, J. Lu, *Nat. Nanotechnol.*, 2022, **17**, 174.

[2] H. Zhang, Y. Zhao, C, Cai, L. Huang, *J. Mater. Chem . A*, 2025, **13**, 37568-37580.